

## First-order Jahn-Teller reduction factors for trigonal complexes

This article has been downloaded from IOPscience. Please scroll down to see the full text article.

1991 J. Phys.: Condens. Matter 3 6845

(<http://iopscience.iop.org/0953-8984/3/35/013>)

View [the table of contents for this issue](#), or go to the [journal homepage](#) for more

Download details:

IP Address: 171.66.16.147

The article was downloaded on 11/05/2010 at 12:31

Please note that [terms and conditions apply](#).

## First-order Jahn–Teller reduction factors for trigonal complexes

J A L Simpson†, C A Bates and J L Dunn

Physics Department, The University, Nottingham NG7 2RD, UK

Received 25 February 1991

**Abstract.** First-order Jahn–Teller reduction factors for strongly coupled orbital triplet systems within trigonal complexes are evaluated. The calculations are based on the model recently proposed by the present authors for such a complex. Detailed results are presented for the reduction factors which correspond to those of  $T \otimes e$  and  $T \otimes t_2$  Jahn–Teller systems in cubic symmetry. It is found that the new factors corresponding to  $T \otimes e$  are virtually unchanged from their cubic counterparts. However, some of the factors derived from the  $T \otimes t_2$  system are changed significantly. The most important change would appear to be that some of the factors remain finite in the strong-coupling limit in contrast to the cubic system where the corresponding factors are completely quenched.

### 1. Introduction

There are many examples known where, on doping a crystal intentionally with impurity ions, the ions do not enter the lattice as simple, isolated, substitutional ions but instead enter the lattice as part of a complex. This situation occurs frequently in the III–V semiconductors such as GaAs, GaP and InP (e.g. Clerjaud 1985). In many such cases, the ion in the complex is very strongly coupled to the vibrations of its surroundings, which therefore complicates any interpretation of the properties of that system. There are also numerous examples of other physical systems (e.g. spinels,  $Al_2O_3$ ) and molecular crystals containing ions in trigonally distorted environments and complexes.

The original motivation for this detailed study of trigonal complexes arose from the need to understand the very complicated optical absorption and photoluminescence spectra observed in various chromium-doped GaAs samples. (This system was technologically important because of the semi-insulating character of the samples produced.) Lack of adequate models caused much confusion in understanding these spectra. The first complex to be clearly identified in this system was  $Cr^{2+}-V_{As}$  (Fujiwara *et al* 1982, Skolnick *et al* 1982), in which one of the As sites surrounding the  $Cr^{2+}$  ion is vacant. One of the current authors was involved in the detailed modelling of this complex (e.g. Barrau *et al* 1983, Austen *et al* 1984, Bates and Brugel 1987, Brugel and Bates 1987), but by treating the vacancy as producing a static trigonal field at the  $Cr^{2+}$  site. Also, Deveaud *et al* (1984) suggested that  $Cr^{2+}-Te$  complexes were formed in GaAs co-doped with Cr and Te. The same complex was also studied by Fujiwara *et al* (1985), and modelling was undertaken by Simpson *et al* (1988). Again, the effect of the Te ion substituting for one of the As ligands was treated by a static trigonal field. Other complexes of Cr in GaAs were subsequently observed, namely  $Cr-V_{As}$ - (Fujiwara *et al* 1986a, b, c) and  $Cr-Se$  (Fujiwara *et al* 1986a).

† Now at: British Aerospace, Sowerby Research Centre, Gold Course Lane, Filton, Bristol BS12 7QW, UK.

More recently, there is interest in the recharging mechanisms involving titanium (Tebbal *et al* 1990) and nickel ions (Erramli *et al* 1991) in various III–V semiconductors. In many of these systems, it is thought that complexes between the magnetic impurity ion and a non-magnetic impurity are formed and could have an important role to play on fixing the equilibrium arrangement in the crystal. Again, it is necessary to have an appropriate model on which these ideas can be tested.

In a recent paper, Simpson *et al* (1990, to be referred to as I) set up and described a model that is generally applicable to strongly coupled orbital triplet ions forming part of a trigonal complex. (By making appropriate changes, the model could be modified readily to apply to octahedral systems as well.) The model in I was based on an initial unitary transformation followed by an energy minimization procedure described previously for cubic symmetry by Bates *et al* (1987), Dunn (1988) and Dunn and Bates (1989). From the model, expressions were obtained for the coordinates of the 13 minima in the potential energy surface, the corresponding eigenstates and their energies. The relationship with the minima for a regular tetrahedron was also discussed.

In order to model the magnetic and optical properties of real complexes, it is necessary to derive an accurate effective Hamiltonian. This means that the associated reduction factors must be calculated. The aim of this paper is to use the model described in I and derive expressions for the first-order reduction factors associated with those seven wells (of tetragonal and trigonal symmetry) which would be associated with the  $T \otimes e$  and  $T \otimes t_2$  Jahn–Teller (JT) systems if the symmetry were increased to cubic. The  $e$  modes  $Q_\theta$  and  $Q_\varepsilon$  of the complex are the same as in the regular tetrahedron. Two types of ‘cubic’  $t_2$  modes are considered, namely those describing radial displacements ( $Q_4, Q_5, Q_6$ ) and those producing transverse displacements ( $Q_7, Q_8, Q_9$ ). The two types of  $t_2$  modes will be considered one at a time. As the actual symmetry is trigonal, it is necessary to define several reduction factors. The orbital states  $T_1$  and  $T_2$  each split into two in trigonal symmetry, namely ( $A_2 + E$ ) and ( $A_1 + E$ ) respectively, while the  $t_2$  vibrations divide into those of  $A_1$  and those of  $E$  symmetry. Each combination of state and mode of vibration has its own reduction factor, which is generally different from other factors. Also included are couplings between the split orbital states.

## 2. Mathematical background for a tetrahedral complex

The trigonal complex consists of a central ion surrounded by four ligands  $i$  ( $i = 1-4$ ), one of which ( $i = 1$ ) is different from the other three in that its charge  $q_1 = (1 + \delta)q$  instead of  $q$  and it is at a distance  $d_1 = (1 + \sigma)d$  from the origin instead of  $d$ . Thus its different charge and/or relative position generates a trigonal distortion in the complex, which is used to define the  $[111]$  axis for the cluster. Neglecting quadratic couplings (which are relatively unimportant except for ‘cubic’  $T \otimes (e + t_2)$  JT systems, which are not being considered here), the total Hamiltonian for an orbital triplet ion coupled to the  $e$  and one of the  $t_2$  modes of the cluster is (I, equations (3.1), (3.7), (3.9))

$$\mathcal{H} = \mathcal{H}_{\text{int}} + \mathcal{H}_{\text{vib}} + \Delta\mathcal{H}_{\text{int}} \quad (2.1)$$

where

$$\begin{aligned} \mathcal{H}_{\text{int}} &= \sum_j K_j r_j (b_j^\dagger + b_j) & j = \theta, \varepsilon; 4, 5, 6 \text{ or } j = \theta, \varepsilon; 7, 8, 9 \\ \mathcal{H}_{\text{vib}} &= \sum_j \hbar\omega_j (b_j^\dagger b_j + \frac{1}{2}) & \Delta\mathcal{H}_{\text{int}} = \frac{1}{4}\delta \sum_j K_j R_j (b_j^\dagger + b_j). \end{aligned} \quad (2.2)$$

In the above,  $\mathcal{H}_{\text{int}}$  is the Hamiltonian for the linear ion–lattice coupling for the regular

tetrahedral cluster,  $\Delta\mathcal{H}_{\text{int}}$  is the additional contribution to the ion–lattice coupling from the trigonal asymmetry and  $\mathcal{H}_{\text{vib}}$  is the Hamiltonian for the vibrations of the cluster. All Hamiltonians are written in terms of second quantized operators; for the orbitals these operators are  $c_n, c_n^\dagger$  ( $n = 1-3$ ) and for the oscillations they are written as  $b_j, b_j^\dagger$ . Combinations  $r_j$  of the orbital operators are used in the above such that  $r_\theta$ , etc., is given by

$$r_\theta = c_1^\dagger c_1 + c_2^\dagger c_2 - 2c_3^\dagger c_3. \tag{2.3}$$

The  $R_j$  operators are trigonal combinations of the  $r_j$  as given in I, equation (3.15). The  $K_j$  are scaled coupling constants such that:

$$K_\theta = K_\varepsilon = K_E \quad K_4 = K_5 = K_6 = K_T \quad K_7 = K_8 = K_9 = K_2 \tag{2.4}$$

while the oscillator frequencies  $\omega_j$  are such that  $\omega_\theta = \omega_\varepsilon = \omega_E, \omega_4 = \omega_5 = \omega_6 = \omega_T$  and  $\omega_7 = \omega_8 = \omega_9 = \omega_2$ .

The procedure adopted in I was to apply a unitary transformation (equation (4.1))

$$U' = \exp\left(i \sum_j \alpha_j' P_j\right) \tag{2.5}$$

to the Hamiltonian  $\mathcal{H}$ , where  $\alpha_j'$  are free parameters for the trigonal cluster and  $P_j'$  are the momenta conjugate to  $Q_j'$ . The transformation has the effect of displacing the origin of each of the oscillators by  $-\alpha_j'/\hbar$ . For strong coupling, the largest part  $\mathcal{H}_1$  of the transformed Hamiltonian  $\mathcal{H}$  does not contain any coupling to excited phonon states. The  $\alpha_j'$  were obtained by minimizing  $\mathcal{H}_1$  with respect to the  $\alpha_j'$ . This is equivalent to obtaining the positions of the minima in the lower potential sheet. A set of coupled equations was obtained, which were expressed in terms of a set of new parameters  $\beta_j$  that are directly related to the  $\alpha_j'$ . After a considerable amount of algebra, the coordinates of the 13 minima ( $k = 1-13$ ) were found and expressed in the form:

$$\alpha_j^{(k)'} = (V_j/\hbar\mu\omega_j)(n_j^{(k)} + \frac{1}{2}\delta'\lambda_j^{(k)}) \tag{2.6}$$

where  $V_j$  derived directly from  $K_j$ . In (2.6),  $\delta'$  ( $= \delta - 4\sigma$ ) represents the total contribution from the trigonal distortion. The values of  $n_j^{(k)}$  and  $\lambda_j^{(k)}$  are given in table 1 of I for both cases of a T ion coupled to one e mode and one  $t_2$  mode (either of the radial or transverse type).

From the analysis, the energies and vibronic ground states in the 13 minima were obtained assuming that the frequencies  $\omega_j$  are comparable in magnitude and that the relative values of the coupling constants  $K_E$  and either  $K_T$  or  $K_2$  could be chosen to produce the required symmetry-type solutions. The results were given in table 2 of I and refined in section 6 of I. For our present purposes, we will consider only those solutions which would reproduce either tetragonal minima and trigonal minima if the trigonal distortion was removed. For convenience, those states and their energies are reproduced in table 1.

In the analysis, only the largest part  $\mathcal{H}_1$  of the transformed Hamiltonian has been included. It is known that the remaining terms are responsible for the anisotropy. This arises from the coupling of the vibronic ground states in the minima to the excited orbital and phonon states in the same well. This problem has been discussed by a number of authors (e.g. Moffitt and Thorson 1957, Bersuker and Polinger 1989, Dunn and Bates 1989) but will be ignored here because it is of secondary importance when compared to the trigonal perturbation.

### 3. The untransformed basis and symmetry-adapted states

The vibronic ground state within one well consists of an orbital part multiplied by an oscillator part with all oscillators having zero excitations. As they stand, these states are

**Table 1.** The corrections to the energies of the wells for the impurity cluster and the corresponding orbital and ground vibronic states for the original cluster. (After Simpson *et al* 1989.)

| Well type  | <i>k</i> | Energy correction        |                          | Orbital states | Ground vibronic states                     |
|------------|----------|--------------------------|--------------------------|----------------|--|
|            |          | Radial                   | Transverse               |                |  |
| Tetragonal | 1-3      | $-\frac{1}{2}\delta'E_E$ | —                        | <i>x, y, z</i> | $ x, 0\rangle,  y, 0\rangle,  z, 0\rangle$ |
| Trigonal   | 4-6      | $-\frac{1}{2}\delta'E_T$ | $-\frac{2}{3}\delta'E_2$ | <i>a, b, c</i> | $ a, 0\rangle,  b, 0\rangle,  c, 0\rangle$ |
|            | 7        | $-\frac{1}{2}\delta'E_T$ | —                        | <i>d</i>       | $ d, 0\rangle$                             |

Definitions

$$\begin{aligned}
 |a\rangle &= (1/\sqrt{3})(+|x\rangle + |y\rangle - |z\rangle) & E_E &= 4K_E^2/\hbar\omega_E \\
 |b\rangle &= (1/\sqrt{3})(+|x\rangle - |y\rangle + |z\rangle) & E_T &= 4K_T^2/3\hbar\omega_T \\
 |c\rangle &= (1/\sqrt{3})(-|x\rangle + |y\rangle + |z\rangle) & E_2 &= 4K_2^2/3\hbar\omega_2 \\
 |d\rangle &= (1/\sqrt{3})(-|x\rangle - |y\rangle - |z\rangle)
 \end{aligned}$$

in a transformed basis as they are centred on the well in question. As all wells must be considered simultaneously, it is necessary to have a common basis for them all. This is achieved by multiplying each vibronic state in each well by the unitary transformation after substitution of the relevant value of  $\alpha'_j$ . Thus the untransformed state  $|X_0^{(k)'}; 0\rangle$  is derived from the transformed state  $|X_0^{(k)}; 0\rangle$  by the relation

$$|X_0^{(k)'}; 0\rangle = U'_k |X_0^{(k)}; 0\rangle$$

with

$$U'_k = \exp\left(\sum_j C_j^{(k)}(b_j - b_j^\dagger)\right) \quad C_j^{(k)'} = -(\frac{1}{2}\mu\hbar\omega_j)^{1/2}\alpha_j^{(k)'}. \quad (3.1)$$

Such states are good eigenstates of the system in the infinite-coupling limit. However, the states in the trigonal minima are not good eigenstates in finite coupling, as the oscillator parts of states in different wells are no longer orthogonal. For these and other reasons, it is necessary to calculate the oscillator overlaps.

$$\begin{aligned}
 S^{kl'} &= \langle 0|(U'_k)^{-1} U'_l|0\rangle \\
 &= \langle 0|\exp\left(\sum_j D_j^{(kl)'}(b_j^\dagger - b_j)\right)|0\rangle = \exp\left(-\frac{1}{2}\sum_j (D_j^{(kl)'})^2\right)
 \end{aligned} \quad (3.2)$$

with

$$D_j^{(kl)'} = C_j^{(k)'} - C_j^{(l)'}$$

for the wells *k* and *l* using the same procedures as those used in Bates *et al* (1987).

For T ⊗ e systems, there is one overlap needed for *k* ≠ *l*, namely

$$S_E^l = S_E(1 + \sigma_E) \quad (3.3)$$

with

$$\sigma_E = -3\delta'(K_E/\hbar\omega_E)^2 \quad S_E = \exp[-6(K_E/\hbar\omega_E)^2].$$

The states  $|x'; 0\rangle (= U'_x|x; 0\rangle)$ ,  $|y'; 0\rangle$  and  $|z'; 0\rangle$  are good eigenstates for all coupling strengths for the trigonal complex as well as the regular cluster where *x*, *y* and *z*

form the orbital basis states written with  $l = 1$ . However, it is necessary to take linear combinations of these states, which are more appropriate for trigonal symmetry. This is very straightforward and the required states are

$$\begin{aligned} |\varphi_{1X}E\rangle &= (1/\sqrt{6})(2|z'; 0\rangle - |x'; 0\rangle - |y'; 0\rangle) \\ |\varphi_{1Y}E\rangle &= (1/\sqrt{2})(|x'; 0\rangle - |y'; 0\rangle) \\ |\varphi_{1Z}A_2\rangle &= (1/\sqrt{3})(|x'; 0\rangle + |y'; 0\rangle + |z'; 0\rangle). \end{aligned} \tag{3.4}$$

The labels in the kets on the left give the symmetry of that state;  $OZ$  is the axis of quantization along  $[111]$  with  $OY$  along  $[110]$ .

For  $T \otimes t_2$  systems, there are two overlaps needed for each of the radial ( $M \equiv T$ ) and transverse modes ( $M \equiv 2$ ) on account of the differences between the wells introduced by the trigonal perturbation. Thus we write the overlaps between the oscillators in the pairs of wells ( $a, b$ ), ( $a, c$ ) and ( $b, c$ ) as  $S'_{Mab}$  (see table 1 for definitions of  $a, b$ , etc.) and between the pairs of wells ( $a, d$ ), ( $b, d$ ) and ( $c, d$ ) as  $S'_{Mad}$ , where

$$S'_{Mab} = S_M(1 + \sigma_{Mab}) \quad S'_{Mad} = S_M(1 + \sigma_{Mad}) \tag{3.5a}$$

with

$$\begin{aligned} S_M &= \exp[-(4K_M/3\hbar\omega_M)^2] \\ \sigma_{Tab} &= -\delta'(4K_T/3\hbar\omega_T)^2(W_4^{(4)} + W_6^{(4)}) & \sigma_{2ab} &= -\delta'(4K_2/3\hbar\omega_2)^2(W_7^{(4)} + W_9^{(4)}) \\ \sigma_{Tad} &= -\delta'(4K_T/3\hbar\omega_T)^2(W_4^{(4)} + W_6^{(7)}) & \sigma_{2ad} &= -\delta'(4K_2/3\hbar\omega_2)^2(W_7^{(4)} + W_9^{(7)}). \end{aligned} \tag{3.5b}$$

In (3.5), the corrections to the overlaps from their cubic counterparts are expressed in terms of the parameters  $W_j^{(k)}$  for well  $k$ , where

$$W_j^{(k)} = \lambda_j^{(k)} / (4n_j^{(k)}) \tag{3.6}$$

with the numerical values of  $\lambda_j^{(k)}$  and  $n_j^{(k)}$  given in table 1 of I. Thus  $j = 4$  and  $6$  is used for the transverse modes and  $j = 7$  and  $9$  for the radial modes.

The required states for the  $T \otimes t_2$  JT problem are found by taking appropriate combinations of the cubic states (Dunn 1988, equations (24) and (30)):

$$\begin{aligned} |T_{1z}t\rangle &= N_{Tt}(-|a'; 0\rangle + |b'; 0\rangle + |c'; 0\rangle - |d'; 0\rangle) \\ |A_2t\rangle &= N_{At}(|a'; 0\rangle + |b'; 0\rangle + |c'; 0\rangle + |d'; 0\rangle) \end{aligned} \tag{3.7}$$

with

$$4N_{Tt}^2(1 + \frac{1}{2}S_T) = 1 \quad 4N_{At}^2(1 - S_T) = 1$$

in the form

$$\begin{aligned} |\Gamma_{1X}M\rangle &= N_{XM}(2|T_{1z}M\rangle - |T_{1z}M\rangle - |T_{1y}M\rangle) \\ |\Gamma_{1Y}M\rangle &= N_{YM}(|T_{1x}M\rangle - |T_{1y}M\rangle) \\ |\Gamma_{1Z}M\rangle &= N_{ZM}(|T_{1x}M\rangle + |T_{1y}M\rangle + |T_{1z}M\rangle) \\ |\Gamma_2M\rangle &= N_{2M}|A_2M\rangle \end{aligned} \tag{3.8}$$

where  $M = T$  or  $2$  as appropriate. ( $|T_{1x}t\rangle$  and  $|T_{1y}t\rangle$  are derived from  $|T_{1z}t\rangle$  above by appropriate cyclic interchanges.) The normalizing constants are given by

$$\begin{aligned} 4N_{2M}^2[3 + S_M(1 + \Omega_{2M})] &= 1 & 8N_{XM}^2[3 + S_M(1 + \Omega_{XM})] &= 1 \\ N_{YM} &= \sqrt{3}N_{XM} & 4N_{2M}^2[1 - S_M(1 + \Omega_{2M})] &= 1 \end{aligned} \tag{3.9}$$

where

$$\begin{aligned}\Omega_{2M} &= -\frac{1}{2}(\sigma_{Mab} - 3\sigma_{Mad} - 8\sqrt{2}\gamma_M) & \Omega_{XM} &= \sigma_{Mab} - 2\sqrt{2}\gamma_M \\ \Omega_{2M} &= \frac{1}{2}(\sigma_{Mab} + \sigma_{Mad})\end{aligned}$$

with  $\gamma_M = -\sqrt{2}\delta'/6$  for the radial modes and  $\gamma_M = +\sqrt{2}\delta'/12$  for the transverse modes.

However, in  $C_{3v}$  symmetry, the states  $|\Gamma_{1Z}M\rangle$  and  $|\Gamma_2M\rangle$  both transform as  $A_2$ . They are therefore not orthogonal, so that a further orthogonal pair of states must be constructed. These states are

$$|\Gamma_aM\rangle = p_a(|\Gamma_{1Z}M\rangle - |\Gamma_2M\rangle) \quad |\Gamma_bM\rangle = p_b(|\Gamma_{1Z}M\rangle + |\Gamma_2M\rangle) \quad (3.10)$$

where

$$\begin{aligned}2p_a^2(1 - A) &= 2p_b^2(1 + A) = 1 \\ A &= \langle \Gamma_{1Z}M | \Gamma_2M \rangle = 2S_M N_{2M} N_{ZM} (-\sigma_{Mab} + \alpha_{Mad} + 4\sqrt{2}\gamma_M).\end{aligned}$$

The states  $|\Gamma_{1X}M\rangle$  and  $|\Gamma_{1Y}M\rangle$  form an E pair and  $|\Gamma_aM\rangle$  and  $|\Gamma_bM\rangle$  are each  $A_2$  singlets.

A further step must be taken because the  $A_2$  states are coupled together by the trigonal parts of the Hamiltonian. Thus the required orthogonal  $A_2$  eigenstates of  $\mathcal{H}_1$  are of the form:

$$\begin{aligned}|\Gamma_\beta M\rangle &= \sin \theta_M |\Gamma_aM\rangle + \cos \theta_M |\Gamma_bM\rangle \\ |\Gamma_aM\rangle &= \cos \theta_M |\Gamma_bM\rangle - \sin \theta_M |\Gamma_\beta M\rangle\end{aligned} \quad (3.11)$$

where

$$\tan 2\theta_M = -2H_{ab}/(H_{aa} - H_{bb}). \quad (3.12)$$

In (3.12),  $H_{aa}$ ,  $H_{bb}$  and  $H_{ab}$  are the matrix elements of  $\mathcal{H}_1$  between the  $A_2$  states labelled by  $b$  and  $a$  as indicated by the subscripts. Thus  $|\Gamma_{1X}M\rangle$ ,  $|\Gamma_{1Y}M\rangle$ ,  $|\Gamma_aM\rangle$  and  $|\Gamma_\beta M\rangle$  can now be used as a suitable basis set of states for the trigonal cluster.

#### 4. Calculation of the reduction factors

Jahn–Teller reduction factors arise when the properties of the ground states of a vibronic system are written in terms of an effective Hamiltonian. Such a procedure is well known and is invoked so that the ground-state energies and the effect of perturbations may be obtained from calculations involving the properties of the orbital operator only. Matrix elements of orbital operators between the ground vibronic states differ from the equivalent matrix elements between the corresponding orbital states by a constant, which is called ‘the first-order reduction factor’. However, in cases in which inversion levels exist, such as in  $T \otimes t_2$ , off-diagonal elements occur that have no ‘pure orbital’ counterpart.

In the calculations to be described here, the so-called second-order reduction factors, which arise from the coupling to excited vibronic states by the perturbation  $V$ , will be omitted. Such calculations have been the subject of detailed calculations recently particularly for  $T \otimes t_2$  JT systems (Bates and Dunn 1989, O’Brien 1990, Dunn *et al* 1990, Polinger *et al* 1991, Bates *et al* 1991). Such terms will undoubtedly be present in trigonal complexes but, to a first approximation, they will be additional to those we derive here and will not interfere with them.

We consider a  $T_1$  ion. In the trigonal complex of  $C_{3v}$  symmetry, the orbital  $T_1$  state splits into an E and an  $A_2$  state. While  $A_1$ ,  $A_2$  and E operators are unchanged by the trigonal perturbation, a  $T_1$  operator is split into an  $A_2$  part, which will be written as

$A_2(T_1)$ , and an E part, to be written as  $E(T_1)$ . Similarly, the trigonal operators derived from the cubic  $T_2$  operator are  $A_1(T_2)$  and  $E(T_2)$ . It is necessary to use trigonal axes as defined in (3.4) for the operators. For example, we have (e.g. Bates 1978)

$$E_\varphi = -(1/\sqrt{2})(l_z l_x + l_x l_z) + \frac{1}{2}(l_+^2 + l_-^2) \tag{4.1}$$

for the E operators, and for the  $T_2$  operators we have

$$\begin{aligned} A_1(T_2) &= \frac{1}{2}[3l_z^2 - l(l+1)] \\ E_\theta(T_2) &= -\frac{1}{2}(l_z l_x + l_x l_z) - \frac{1}{2}\sqrt{2}(l_+^2 + l_-^2). \end{aligned} \tag{4.2}$$

For  $T_1$  operators, we have  $l_z$  for  $A_2(T_1)$  and  $l_x, l_y$  for  $E(T_1)$ . It should be noted that difficulties can arise when matrix elements are evaluated between vibronic states that have no orbital counterpart in devising an appropriate formalism for their display.

#### 4.1. The $T \otimes e$ system

As stated above, the reduction factor  $K_{\Gamma\Omega}^e[\Omega(P)]$  for an operator  $\mathcal{P}$  of symmetry P may be found by comparing the matrix elements of  $\mathcal{P}$  within the set of vibronic states of symmetry  $\Gamma, \Omega$  given in (3.4) with the matrix elements of  $\mathcal{P}$  within the corresponding pure orbital states. (The superscript ‘e’ is used to label the  $\pi$  system discussed here; the label ‘t’ will be used below for the  $T \otimes t_2$  system.) For example,

$$K_{A_2A_2}^e[E(T_1)] = \frac{\langle \varphi_{1z} A_2 | A_1(T_2) | \varphi_{1z} A_2 \rangle}{\langle Z | A_1(T_2) | Z \rangle} \tag{4.3}$$

Detailed calculations give the following results:

$$\begin{aligned} K_{EE}^e[E(E)] &= K_{A_2A_2}^e[E(E)] = 1 \\ K_{A_2A_2}^e[A_1(T_2)] &= K_{EE}^e[A_1(T_2)] = K_{EA_2}^e[E(T_1)] = K_{EE}^e[A_2(T_1)] \\ &= K_{EA_2}^e[E(T_2)] = K_{EE}^e[E(T_2)] = S_E'. \end{aligned} \tag{4.4}$$

These results are very similar to those obtained in the regular cluster with the oscillator overlap  $S_E'$  for the complex replacing the standard oscillator overlap  $S_E$ . Complete quenching thus occurs in the infinite-coupling limit for six of the reduction factors. The reduction factors are plotted as a function of  $(K_E/\hbar\omega_E)$  in figure 1 with  $\delta' = 0.1$ . For comparison, the reduction factor ( $= S_E$ ) for the regular cluster is also included in the figure.

#### 4.2. The $T \otimes t_2$ system

This situation is much more complicated than the  $T \otimes e$  and regular  $T \otimes t_2$  systems as there are many more independent factors and operators to be taken into account. The calculation proceeds in exactly the same way as that for  $T \otimes e$  using the vibronic states given in (3.8) and (3.11). In order to organize the results, the reduction factors will be grouped according to their regular counterparts, namely  $K^t(E)$ ,  $K^t(T_1)$  and  $K^t(T_2)$ . Details of the calculation and the results are given in the appendix.

The reduction factor  $K^t(E)$  for the regular cluster is divided into three independent factors for the complex as given in equations (A1) and (A2).  $K^t(T_1)$  also divides into three, of which there is one labelled as  $A_2(T_1)$ , and given in (A4), and two under the label  $E(T_1)$  given in (A5). It is necessary to take  $K^t(T_2)$  and  $\langle T_1 | T_2 | A_2 \rangle$  together; there are four factors labelled by  $A_1(T_2)$  (equation (A6)) and three by  $E(T_2)$  (equation (A7)).



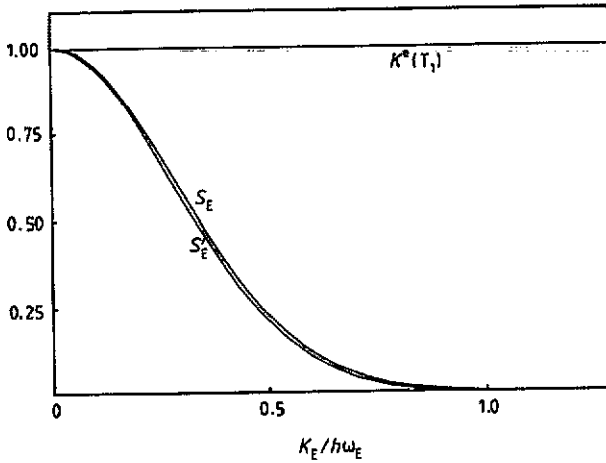


**Figure 1.** The  $T \otimes e$  reduction factors plotted as a function of  $(K_E/\hbar\omega_E)$  with  $\delta' = 0.1$  as given in (4.4). The regular factors  $K^e(E) = 1$  and  $K^e(T_1) = K^e(T_2) = K_{EE}^e = K_{\lambda_2 A_2}^e = S_E$  are also shown for comparison purposes.

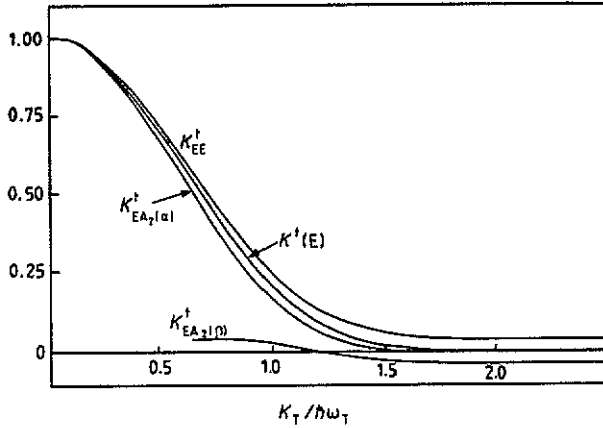


**Figure 2.** The  $E(E)$  reduction factors for  $T \otimes t_2$  radial modes plotted as a function of  $(K_T/\hbar\omega_T)$  with  $\delta' = 0.1$  as given by (A1) and (A2). The corresponding regular reduction factor  $K^t(E)$  is also shown for comparison purposes.

In the following discussion, coupling to radial  $t_2$  modes only is discussed in detail. Results for the transverse modes will have an equivalent form.

**4.2.1. Derivatives of  $K^t(E)$ .** The three  $E(E)$  reduction factors are plotted against the coupling strength  $(K_T/\hbar\omega_T)$  for the radial modes in figure 2 for  $\delta' = 0.1$ . For comparison purposes,  $K^t(E)$  is also plotted. The figure shows that, in the strong-coupling limit,  $K_{EE}^t[E(E)]$  and  $K_{EA_2(\beta)}^t[E(E)]$  tend to the limit of magnitude  $\sqrt{2} \gamma_M$  while  $K_{EA_2(\alpha)}^t[E(E)]$  is completely quenched. [These results for the strong coupling limit can also be derived directly from equations (A1) and (A2) as  $S_M \rightarrow 0$ ,  $b_1 \rightarrow \frac{2}{3}\sqrt{2} \gamma_M$  and  $N_{XM}^2 \rightarrow 1/24$  (from (3.9)). Substitution in the formulae reproduces the above results.]

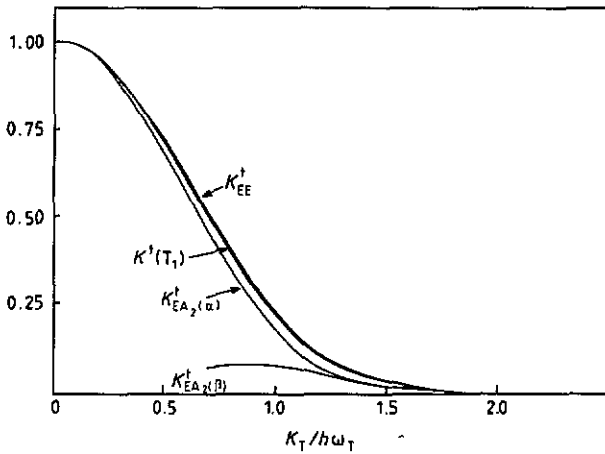


Figure 3. The  $A_2(T_1)$  and  $E(T_1)$  reduction factors for the radial modes of the  $T \otimes t_2$  trigonal complex plotted as a function of  $(K_T/\hbar\omega_T)$  with  $\delta' = 0.1$ .  $K^t(T_1)$  is also plotted for comparison purposes.

The non-zero limit for the first two cases can be anticipated as the trigonal field mixes some  $E(T_2)$ -type characteristics into the  $E(E)$  operators. As cubic  $T_2$ -type operators are only partially quenched in the strong-coupling limit, admixtures of them result in a non-zero limit as observed. When  $(K_T/\hbar\omega_T)$  tends to zero, the reduction factor  $K^t_{EA_2(\alpha)}[E(E)]$  can be approximated to  $L(E)_T$ . This is, in turn, consistent with the use of the first three ground basis states given in (3.8) as approximate eigenstates of the system provided the coupling to the other excited  $A_2$  singlet  $|\Gamma_2M\rangle$  can be ignored. The two other reduction factors both tend to unity in this limit.

In the limit of  $\delta'$  tending to zero, both  $I(E)_M$  and  $K^t_{EA_2(\beta)}[E(E)]$  vanish as the coupling of the trigonal field to the excited singlet state goes to zero, and the reduction factors  $K^t_{EE}[E(E)]$  and  $K^t_{EA_2(\alpha)}[E(E)]$  both become equal to  $K^t(E)$  of the regular cluster where (e.g. Bates and Dunn 1989)

$$K^t(E) = 4S_T/(3 + S_T). \tag{4.5}$$

4.2.2. *Derivatives of  $K^t(T_1)$ .* The  $A_2(T_1)$  and  $E(T_1)$  reduction factors for the radial modes are plotted, together with  $K^t(T_1)$ , in figure 3 with  $\delta' = 0.1$ . The graphs show that  $A_2(T_1)$  and  $E(T_1)$  are each completely quenched in the very-strong-coupling limit as with  $K^t(T_1)$ . In the weak-coupling limit,  $L(1)_M$  can be used as an approximate reduction factor between the  $E(T_1)$  doublet and  $A_2(T_1)$  singlet for the same reasons as above. Both  $K^t_{EE}[A_2(T_1)]$  and  $L(1)_M$  tend to unity as the coupling tends to zero.

In the other limiting case when  $\delta'$  tends to zero,  $I(1)_M$  and  $K^t_{EA_2(\beta)}[E(T_1)]$  both tend to zero as the coupling of the trigonal field to the excited singlet state disappears. Thus  $K^t_{EE}[A_2(T_1)]$  and  $K^t_{EA_2(\alpha)}[E(T_1)]$  both tend to  $K^t(T_1)$ .

4.2.3. *Derivatives of  $K^t(T_2)$ .* The  $A_1(T_2)$  and  $E(T_2)$  reduction factors are more complicated as there are more of them. The results for the radial modes are plotted in figures 4(a) and (b) with  $\delta' = 0.1$  as before together with their cubic counterparts  $K^t(T_2)$  and  $\langle A_2|T_2|T_1\rangle$ . In the very-strong-coupling limit, the reduction factors have the following values:

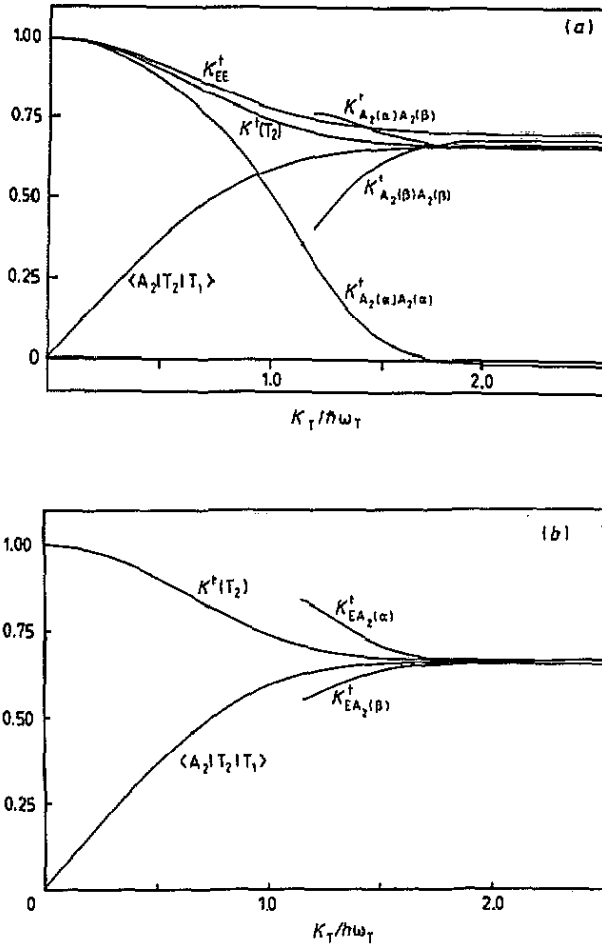


Figure 4. (a) The  $A_1(T_2)$  and (b) the  $E(T_2)$  reduction factors for the radial modes of the  $T \otimes t_2$  trigonal complex plotted as a function of  $(K_T/\hbar\omega_T)$  with  $\delta' = 0.1$ . Their cubic counterparts of  $K^{\dagger}(T_2)$  and  $\langle A_2|T_2|T_1 \rangle$  are also shown. Note that in (b),  $K_{EE}^{\dagger}[E(T_2)]$  is not shown separately as it cannot be distinguished from the curve for  $K^{\dagger}(T_2)$  with the scale used.

$$\begin{aligned}
 K_{EE}^{\dagger}[A_1(T_2)] &= \frac{2}{3}(1 - 2\sqrt{2} \gamma_T) & K_{A_2(\alpha)A_2(\alpha)}^{\dagger}[A_1(T_2)] &= \frac{1}{3}\sqrt{2} \gamma_T \\
 K_{A_2(\beta)A_2(\beta)}^{\dagger}[A_1(T_2)] &= \frac{2}{3}(1 - \frac{1}{3}\sqrt{2} \gamma_T) \\
 K_{A_2(\alpha)A_2(\beta)}^{\dagger}[A_1(T_2)] &= K_{EE}^{\dagger}[E(T_2)] = K_{EA_2(\alpha)}^{\dagger}[E(T_2)] \\
 &= K_{EA_2(\beta)}^{\dagger}[E(T_2)] = \frac{2}{3}(1 + \frac{1}{3}\sqrt{2} \gamma_T).
 \end{aligned}
 \tag{4.6}$$

If the coupling to the excited  $A_2$  state is neglected and  $(K_M/\hbar\omega_M)$  tends to zero, the reduction factors  $K_{A_2(\alpha)A_2(\alpha)}^{\dagger}[A_1(T_2)]$  and  $K_{EA_2(\alpha)}^{\dagger}[E(T_2)]$  can be approximated by  $L(T)_M$  and  $L(T')_M$  respectively. These approximate factors, together with  $K_{EE}^{\dagger}[A_1(T_2)]$ , are well defined and tend to unity as the coupling strength tends to zero.

In the limit when  $\delta'$  tends to zero, the factor  $K_{A_2(\alpha)A_2(\alpha)}^{\dagger}[A_1(T_2)]$  tends to zero, while

the magnitudes of  $K_{A_2(\beta)A_2(\alpha)}^t[A_2(T_2)]$  and  $K_{A_2(\alpha)A_2(\alpha)}^t[E(T_2)]$  reduce to the value of the regular element  $\langle A_2|T_2|T_1 \rangle$ , which is given by (Bates and Dunn 1989)

$$\langle A_2|T_2|T_1 \rangle = \frac{2}{3}[(1 - S_T)/(1 + \frac{1}{3}S_T)]^{1/2}. \quad (4.7)$$

The remaining reduction factors involving the doublet  $E(T_1)$  and the singlet  $A_2(T_1)$  states tend to the cubic reduction factor  $K^t(T_2)$  where (Bates and Dunn 1989)

$$K^t(T_2) = 2(1 + S_T)/(3 + S_T). \quad (4.8)$$

## 5. Discussion and conclusions

This paper has described calculations of the first-order reduction factors that have been undertaken for a trigonal cluster. It has concentrated on those systems which would be described as  $T \otimes e$  and  $T \otimes t_2$  if the trigonal distortion was removed. The method adopted has used the symmetry-adapted states given in equations (3.4), (3.8) and (3.10). These states were derived from the transformed states located in the various minima in the potential energy surface. The latter were obtained from the original calculations of Simpson *et al* (1990) using an initial unitary transformation. The formalism developed in this model has been shown to be convenient to use. To our knowledge, no other calculations of these reduction factors exist in the literature which take into account the trigonal nature of the ion-lattice interaction.

The results for those reduction factors which are derived from the cubic  $T \otimes e$  JT system and shown in figure 1 clearly show that the trigonal perturbation has very little effect and could be ignored in virtually all calculations. However, some of the reduction factors for the trigonal complex do differ in some important ways from their cubic counterparts in  $T \otimes t_2$  JT systems. Among the most significant is that  $K_{E(E)}^t[E(E)]$  and  $K_{EA_2(\beta)}^t[E(E)]$  tend to a finite value of  $\sqrt{2} \gamma_M$  in the infinite-coupling limit rather than the limiting value of zero for the cubic case. In a similar way, all seven of the trigonal  $A_1(T_2)$  and  $E(T_2)$  reduction factors deviate from their cubic infinite-coupling limits by a multiple of  $\gamma_M$  as shown in figures 4(a) and (b). In some cases, the deviation is from the value of  $\frac{2}{3}$  while in other cases the deviation is from zero. In all cases, deviations in weak coupling (e.g.  $K_M/\hbar\omega_M$  less than unity) between the trigonal and cubic factors as shown in figures 2-4 are not always reliable as the states are not designed for this region.

The departures of some of the reduction factors from their cubic infinite-coupling limits is the most significant of the results described here. It is important to take this into account in the modelling of experimental data on real systems, many of which are not cubic. Thus the identification of the type of the dominant JT coupling should proceed with care.

We note also that some progress has been made in deriving the reduction factors for orthorhombic  $T \otimes (e + t_2)$  JT systems within trigonal complexes. However, the results are even more complicated than those for  $T \otimes t_2$  because of the difficulty of accurately modelling both split and coupled triplets ( $T_1 + T_2$ ) in a compact form when the coupling is to two e and one  $a_1$  modes.

Work is currently in progress to use the theory for complexes derived above to model all the complexes of Cr in GaAs described in the introduction.

## Acknowledgment

One of us (JLS) wishes to thank the SERC for a research studentship.

## Appendix. Reduction factors for $T \otimes t_2$

There are 13 reduction factors, which may be classified under their cubic counterparts.

### A.1. Derivatives from the cubic $K^i(E)$ reduction factors

There are three independent reduction factors each described by  $E(E)$ . Within the vibronic doublet, we have one, namely

$$K_{EE}^1[E(E)] = 32N_{XM}^2(a_1S_M + b_1) \quad (A1)$$

where

$$a_1 = 1 + \sigma_{Mab} + \frac{1}{4}\sqrt{2}\gamma_M \quad b_1 = -\frac{3}{4}\sqrt{2}\gamma_M.$$

The other reduction factors are between the doublet and each of the two singlets. They are

$$\begin{aligned} K_{EA_2(\alpha)}^1[E(E)] &= \mu_1 L(E)_M - \mu_2 I(E)_M \\ K_{EA_2(\beta)}^1[E(E)] &= \mu_3 L(E)_M + \mu_4 I(E)_M \end{aligned} \quad (A2)$$

where

$$\begin{aligned} \mu_1 &= p_a \cos \theta_M - p_b \sin \theta_M & \mu_2 &= p_a \cos \theta_M + p_b \sin \theta_M \\ \mu_3 &= p_b \cos \theta_M + p_a \sin \theta_M & \mu_4 &= p_b \cos \theta_M - p_a \sin \theta_M. \end{aligned}$$

The quantities  $L(E)_M$  and  $I(E)_M$  are the component factors associated with  $\langle \Gamma_{12}M | E_\theta | \Gamma_{1X}M \rangle$  and  $\langle \Gamma_{1X}M | E_\theta | \Gamma_{2M} \rangle$ . They have the values

$$\begin{aligned} L(E)_M &= 16\sqrt{2} N_{ZM} N_{XM} (a_2 S_M + b_2) \\ I(E)_M &= 4\sqrt{2} N_{XN} N_{2M} [(3/\sqrt{2})\gamma_M + S_M(\sigma_{Mad} - \sigma_{Mad} + \frac{1}{2}\sqrt{2}\gamma_M)] \end{aligned} \quad (A3)$$

where

$$a_2 = 1 + \frac{1}{4}(\sigma_{Mab} + 3\sigma_{Mad}) - \frac{1}{8}\sqrt{2}\gamma_M \quad b_2 = \frac{3}{8}\sqrt{2}\gamma_M.$$

### A.2. Derivatives from the $K^i(T_1)$ reduction factors

A.2.1. *The  $A_2(T_1)$  reduction factor.* There is one  $A_2(T_1)$  reduction factor which operates within the  $E$  states, namely

$$K_{EE}^1[A_2(T_1)] = 32N_{XM}^2 S_M [1 + \sigma_{Mab} - \frac{1}{2}\sqrt{2}\gamma_M]. \quad (A4)$$

A.2.2. *The  $E(T_1)$  reduction factor.* There are two reduction factors of symmetry  $E(T_1)$  as there are two  $A_2$  states. Thus

$$\begin{aligned} K_{EA_2(\beta)}^1[E(T_1)] &= \mu_1 L(I')_M - \mu_2 I(I')_M \\ K_{EA_2(\alpha)}^1[E(T_1)] &= \mu_3 L(I')_M + \mu_4 I(I')_M \end{aligned} \quad (A5)$$

where

$$\begin{aligned} L(I')_M &= 16\sqrt{2} N_{XM} N_{ZM} S_M [1 + \frac{1}{4}(\sigma_{Mab} + 3\sigma_{Mad}) + \frac{1}{4}\sqrt{2}\gamma_M] \\ I(I')_M &= 8\sqrt{2} N_{XM} N_{2M} S_M [\sqrt{2}\gamma_M + \frac{1}{2}(\sigma_{Mab} - \sigma_{Mad})]. \end{aligned}$$

The quantities  $L(I')_M$  and  $I(I')_M$  are derived from calculating  $\langle \Gamma_{1X}M | l_Y | \Gamma_{1Z}M \rangle$  and  $\langle \Gamma_{1X}M | l_Y | \Gamma_{2Z}M \rangle$  respectively, for example.

### A.3. Derivatives from the cubic $K'(T_2)$ and $\langle T_1 | T_2 | A_2 \rangle$ reduction factors.

A.3.1. The  $A_1(T_2)$  reduction factors. There are four  $A_1(T_2)$  reduction factors. They are

$$\begin{aligned} K_{EE}^1[A_1(T_2)] &= 16N_{XM}^2[S_M(1 + \sigma_{Mab} + \sqrt{2}\gamma_M) + (1 - 2\sqrt{2}\gamma_M)] \\ K_{A_2(\alpha)A_2(\alpha)}^1[A_1(T_2)] &= \mu_1^2L(T)_M - 2\mu_1\mu_2I(T)_M + \mu_2^2J(T)_M \\ K_{A_2(\beta)A_2(\beta)}^1[A_1(T_2)] &= \mu_3^2L(T)_M + 2\mu_3\mu_4I(T)_M + \mu_4^2J(T)_M \\ K_{A_2(\alpha)A_2(\beta)}^1[A_1(T_2)] &= \mu_1\mu_3L(T)_M - \mu_2\mu_4J(T)_M + (\mu_1\mu_4 - \mu_2\mu_3I(T)_M) \end{aligned} \quad (A6)$$

where

$$\begin{aligned} L(T)_M &= 8N_{ZM}^2\{S_M[1 + \frac{1}{4}(\sigma_{Mab} + 3\sigma_{Mad}) + \frac{1}{4}\sqrt{2}\gamma_M] + (1 + \frac{1}{4}\sqrt{2}\gamma_M)\} \\ I(T)_M &= 4N_{ZM}N_{2M}\{(1 - \frac{1}{2}\sqrt{2}\gamma_M) - S_M[1 + \frac{1}{2}(\sigma_{Mab} + \sigma_{Mad}) + \frac{3}{2}\sqrt{2}\gamma_M]\} \\ J(T)_M &= -2N_{2M}^2[\sqrt{2}\gamma_M + S_M(\sigma_{Mab} - \sigma_{Mad} - \sqrt{2}\gamma_M)]. \end{aligned}$$

$L(T)_M$ ,  $I(T)_M$  and  $J(T)_M$  are calculated from  $\langle \Gamma_{1Z}M | A_1(T_2) | \Gamma_{1Z}M \rangle$ ,  $\langle \Gamma_{1Z}M | A_1(T_2) | \Gamma_{2Z}M \rangle$  and  $\langle \Gamma_{2Z}M | A_1(T_2) | \Gamma_{2Z}M \rangle$  respectively.

A.3.2. The  $E(T_2)$  reduction factors. There are three factors, as follows:

$$\begin{aligned} K_{EE}^1[E(T_2)] &= 16N_{XM}^2[S_M(1 + \sigma_{Mab} - \frac{3}{4}\sqrt{2}\gamma_M) + (1 + \frac{1}{4}\sqrt{2}\gamma_M)] \\ K_{EA_2(\alpha)}^1[E(T_2)] &= \mu_1L(T')_M - \mu_2I(T')_M \\ K_{EA_2(\beta)}^2[E(T_2)] &= \mu_3L(T')_M + \mu_4I(T')_M. \end{aligned} \quad (A7)$$

The quantities  $L(T')_M$  and  $I(T')_M$  are obtained, for example, from evaluating  $\langle \Gamma_{1X}M | E_\theta(T_2) | \Gamma_{1Z}M \rangle$  and  $\langle \Gamma_{1X}M | E_\theta(T_2) | \Gamma_{2Z}M \rangle$  respectively, where  $E_\theta(T_2)$  is given in equation (4.2). The results are

$$\begin{aligned} L(T')_M &= 8\sqrt{2}(N_{XM}N_{ZM})\{[1 - \frac{1}{2}(\sigma_{Mab} - 3\sigma_{Mad}) + \frac{1}{4}\sqrt{2}\gamma_M]S_M + (1 + \frac{1}{4}\sqrt{2}\gamma_M)\} \\ I(T')_M &= -8\sqrt{2}(N_{XM}N_{2M})\{-[1 + \frac{1}{2}(\sigma_{Mab} + \sigma_{Mad}) - \frac{3}{4}\sqrt{2}\gamma_M]S_M + (1 + \frac{1}{4}\sqrt{2}\gamma_M)\}. \end{aligned} \quad (A8)$$

## References

- Austen S P, Bates C A and Brugel D 1984 *J. Phys. C: Solid State Phys.* **17** 1257–68  
 Barrau J, Brousseau M, Austen S P and Bates C A 1983 *J. Phys. C: Solid State Phys.* **16** 4581–98  
 Bates C A 1978 *Phys. Rep.* **35** 187–304  
 Bates C A and Brugel D 1987 *Semicond. Sci. Technol.* **2** 494–500  
 Bates C A and Dunn J L 1989 *J. Phys.: Condens. Matter* **1** 2605–16  
 Bates C A, Dunn J L, Hallam L D, Kirk P J and Polinger V Z 1991 *J. Phys.: Condens. Matter* **3** 3441–53  
 Bates C A, Dunn J L and Sigmund E 1987 *J. Phys. C: Solid State Phys.* **20** 1965–83 (corrigenda 1987 **20** 4015)  
 Bersuker I B and Polinger V Z 1989 *Vibronic Interactions in Molecules and Crystals* (Berlin: Springer)  
 Brugel D and Bates C A 1987 *Semicond. Sci. Technol.* **2** 501–6  
 Clerjaud B 1985 *J. Phys. C: Solid State Phys.* **18** 3615–61  
 Deveaud B, Lambert B, Picoli G and Martinez G 1984 *J. Appl. Phys.* **55** 4356–60

- Dunn J L 1988 *J. Phys. C: Solid State Phys.* **21** 383-99
- Dunn J L and Bates C A 1989 *J. Phys: Condens. Matter* **1** 375-94
- Dunn J L, Bates C A and Kirk P J 1990 *J. Phys.: Condens. Matter* **2** 10379-89
- Erramli A, Al-Ahmadi M S G, Ulrici W, Tebbal N, Krissl J, Vasson A-M, Vasson A and Bates C A 1991 *J. Phys.: Condens. Matter* **3** 6345-62
- Fujiwara Y, Kita Y, Tonami Y, Nishimo T and Hamakawa Y 1986a *Japan J. Appl. Phys.* **25** L232-4
- 1986b *Proc. Int. Conf. Semi-Insulating III-V Materials (Japan)* (Tokyo: Ohmsha) pp 115-20
- 1986c *J. Phys. Soc. Japan* **55** 3741-4
- Fujiwara Y, Kojima A, Nishino T and Hamakawa Y 1985 *J. Appl. Phys.* **24** 1479-83
- Fujiwara Y, Nishino T and Hamakawa Y 1982 *Japan. J. Appl. Phys.* **21** L379
- Moffitt W and Thorson W 1957 *Phys. Rev.* **108** 1251-5
- O'Brien M C M 1990 *J. Phys.: Condens. Matter* **2** 5539-53
- Polinger V Z, Bates C A and Dunn J L 1991 *J. Phys.: Condens. Matter* **3** 513-27
- Simpson J L, Bates C A, Barrau J, Brousseau M and Thomas V 1988 *Semicond. Sci. Technol.* **3** 178-84
- Simpson J L, Dunn J L and Bates C A 1990 *J. Phys.: Condens. Matter* **2** 8315-26
- Skolnick M S, Brozel M R and Tuck B 1982 *Solid State Commun.* **43** 379-84
- Tebbal N, Vasson A-M, Vasson A, Erramli A and Ulrici W 1990 *J. Phys.: Condens. Matter* **2** 7907-10